AGU PUBLICATIONS

Geophysical Research Letters

RESEARCH LETTER
10.1002/2015GL066476

**Key Points:**
- Katabatic winds have scoured unconformities in the internal annual layers of the Blue Ice Area (BIA)
- Unconformities evidence paleo BIA and represent breaks in the paleo climate record
- Ground-penetrating radar should be used to examine BIA and interpret climate records

**Correspondence to:**
K. Winter,
kate.winter@northumbria.ac.uk;
katewinter15@gmail.com

**Citation:**
Winter, K., et al. (2016), Assessing the continuity of the blue ice climate record at Patriot Hills, Horseshoe Valley, West Antarctica, *Geophys. Res. Lett., 43*, 2019–2026, doi:10.1002/2015GL066476.

Received 6 OCT 2015
Accepted 11 FEB 2016
Accepted article online 13 FEB 2016
Published online 2 MAR 2016



# Assessing the continuity of the blue ice climate record at Patriot Hills, Horseshoe Valley, West Antarctica

**Kate Winter[1], John Woodward[1], Stuart A. Dunning[2], Chris S. M. Turney[3], Christopher J. Fogwill[3], Andrew S. Hein[4], Nicholas R. Golledge[5], Robert G. Bingham[4], Shasta M. Marrero[4], David E. Sugden[4], and Neil Ross[2]**

[1]Department of Geography, Faculty of Engineering and Environment, Northumbria University, Newcastle upon Tyne, UK, [2]School of Geography, Politics and Sociology, University of Newcastle upon Tyne, Newcastle upon Tyne, UK, [3]Climate Change Research Centre, School of Biological, Earth and Environmental Sciences, University of New South Wales, Kensington, New South Wales, Australia, [4]School of GeoSciences, University of Edinburgh, Edinburgh, UK, [5]Antarctic Research Centre, Victoria University of Wellington, Wellington, New Zealand

**Abstract** We use high-resolution ground-penetrating radar (GPR) to assess the continuity of the Blue Ice Area (BIA) horizontal climate record at Patriot Hills, Horseshoe Valley, West Antarctica. The sequence contains three pronounced changes in deuterium isotopic values at ~18 cal ka, ~12 cal ka, and ~8 cal ka. GPR surveys along the climate sequence reveal continuous, conformable dipping isochrones, separated by two unconformities in the isochrone layers, which correlate with the two older deuterium shifts. We interpret these unconformities as discontinuities in the sequence, rather than direct measures of climate change. Ice sheet models and Internal Layer Continuity Index plots suggest that the unconformities represent periods of erosion occurring, as the former ice surface was scoured by katabatic winds in front of mountains at the head of Horseshoe Valley. This study demonstrates the importance of high-resolution GPR surveys for investigating both paleoflow dynamics and interpreting BIA climate records.

## 1. Introduction

With a capacity to resolve internal layering within ice, ground-penetrating radar (GPR) has transformed our ability to study and interpret historic changes in ice flow [*Paren and Robin*, 1975; *Daniels et al*., 1988; *Fujita et al*., 1999; *Rippin et al*., 2003, 2006; *Woodward and King*, 2009; *Sime et al*., 2011; *Drews et al*., 2013]. Despite this, there is limited analysis of the detailed internal structure of Blue Ice Areas (BIAs), which are estimated to cover 120,000 km$^2$ (~0.8%) of the Antarctic continent [*Winther et al*., 2001]. This is perhaps a function of the reduced performance of conventional snowmobile towed GPR surveys in these areas [*Spaulding et al*., 2013; *Turney et al*., 2013], where the speed of travel results in a reduced scan rate relative to the distance traveled, which reduces the ability to image the detailed internal strata of BIAs. Defined as regions of exposed ice with a relatively low surface albedo [*Bintanja*, 1999], BIAs typically form on the leeward foreground of mountain ranges, where upward ice flow around the mountains and/or into the mountain front compensates for surface ablation (similar to erosion-induced bedrock uplift in mountains). This allows deeper, older ice to rise toward the surface where it is exposed, typically as a rippled blue ice surface [*Bintanja*, 1999; *Sinisalo and Moore*, 2010; *Fogwill et al*., 2012; *Campbell et al*., 2013]. This phenomenon enables old ice to be exposed, enabling "ice sequence" climate records to be collected along the BIA surface [*Whillans and Cassidy*, 1983; *Korotkikh et al*., 2011; *Fogwill et al*., 2012; *Spaulding et al*., 2012; *Spaulding et al*., 2013; *Turney et al*., 2013]. So-called "horizontal coring" offers considerable logistical benefits over vertical coring, although such climate records require careful interpretation, as the processes that have brought packages of ice to the surface may impact upon their continuity and therefore their paleo significance.

Here we use commercial GPR in step-and-collect mode to analyze, in detail, the internal structure of Patriot Hills BIA, in Horseshoe Valley, West Antarctica (80°18′S, 81°21′W; Figure 1). We compare this high-resolution BIA GPR data set, capable of recording zones of continuous and discontinuous isochrones and their dip angles, to deuterium-isotope-derived late Pleistocene/early Holocene climate records [*Turney et al*., 2013] to aid climate record interpretations. Model simulations and englacial stratigraphy continuity plots from airborne radio echo sounding of the Institute and Möller Ice Streams [*Bingham et al*., 2015; *Winter et al*., 2015] are also used to investigate the history and evolution of ice sheet flow in Horseshoe Valley.

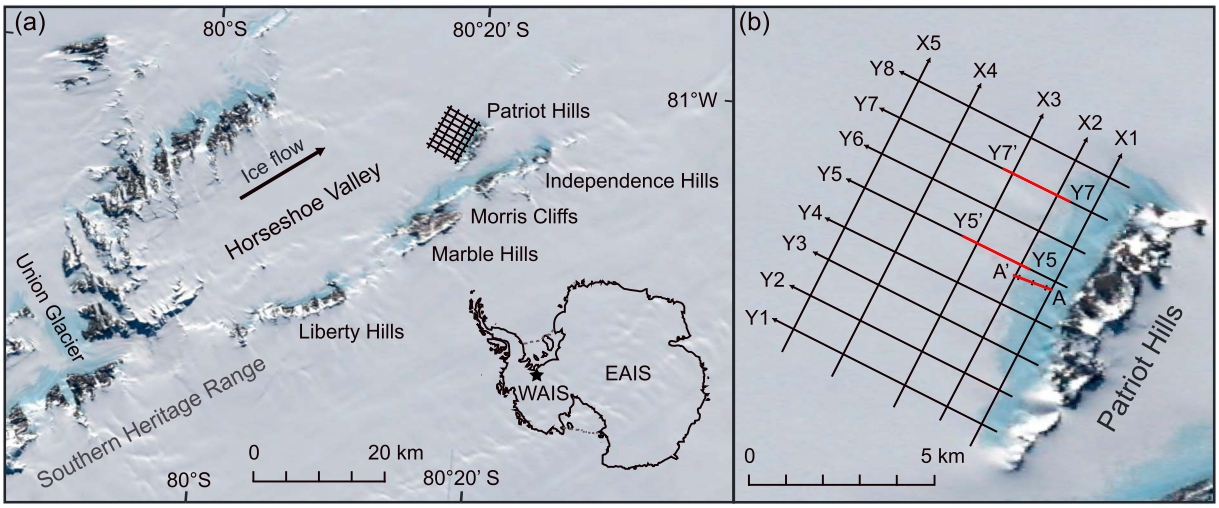


**Figure 1.** (a) Moderate Resolution Imaging Spectroradiometer (MODIS) mosaic [*Haran et al*., 2006] showing the location of Patriot Hills, Horseshoe Valley (marked with a star on the wider Antarctic setting). Ice flows from the head of the Horseshoe Valley toward Patriot Hills. (b) Zoom in of the nested ground-penetrating radar grid (X1–X5 and Y1–Y8) and the climate transect (A), where ice flows up toward the Blue Ice Area surface. Red lines show the location and extent of ground-penetrating radar profiles used in this paper. Arrows show direction of data collection away from the mountains (A and Y1–Y8) and down valley (X1–X5).

## 2. Methods

### 2.1. Ground-Penetrating Radar

A PulseEKKO 1000 GPR system was used to generate a 200 MHz GPR profile along a central BIA transect, extending perpendicular to Patriot Hills for 800 m, along the climate record (Transect A, Figure 1). To obtain a high-resolution GPR profile, we employed continuous step-and-collect mode with a 7000 ns time window and an in-field stack of 8. The GPR data were collected at 0.1 m intervals with copolarized antennae orientated perpendicular to the survey line, with their broadsides parallel to each other. This time-intensive method is described in detail by *Woodward et al*. [2001]. A further nested grid of high-frequency lines (approximately $7 \times 9$ km with 1 km $\times$ 1.5 km grid cells) extending from the BIA margin (Figure 1) was also surveyed in 2014 by towing the sledge-mounted PulseEKKO 1000 system by snowmobile at approximately 12 km/h along each transect line with no in-field stacking. This mode of operation is much faster than step-and-collect mode, allowing a larger area to be surveyed, albeit at a reduced resolution. Each line was surveyed for topographic correction using a Trimble differential GPS unit and corrected to decimeter accuracy using a local base station. GPR data were processed in Reflexw [*Sandmeier Scientific Software*, 2012], version 6.1.1., using standard processing steps [*Welch and Jacobel*, 2005; *Woodward and King*, 2009; *King*, 2011]. These steps include time-zero correction, background removal, high-pass frequency filtering (Dewow), band-pass filtering, and diffraction-stack migration. An energy-decay gain was also applied. For display purposes depth and topographic corrections were applied using an ice velocity of 0.168 m ns$^{-1}$. Applying this standard velocity underestimates the depth of firn layers away from the BIA.

### 2.2. Ice Sheet Model Simulations

Preexisting ice sheet model perturbation experiments [*Golledge et al*., 2012; *Fogwill et al*., 2014] were used to investigate ice flux and ice flow direction in Horseshoe Valley during the Holocene. The Parallel Ice Sheet Model (PISM) is a three-dimensional, thermomechanical, continental ice sheet model that combines shallow-ice and shallow-shelf approximation equations in order to simulate the dynamic behavior of grounded ice, floating ice, and ice streams. Model runs used proxy-based interpretations of atmospheric [*Petit et al*., 1999] and oceanic [*Lisiecki and Raymo*, 2005; *Imbrie and McIntyre*, 2006] changes during the last glacial cycle and employ boundary conditions from modified Bedmap topography [*Le Brocq et al*., 2010], as well as a spatially varying geothermal heat flux interpolation [*Shapiro and Ritzwoller*, 2004]. Our perturbation experiments were run at a resolution of 5 km, starting from a Last Glacial Maximum (LGM) (occurring sometime between 29 and 33 ka in West Antarctica) [*Clark et al*., 2009] configuration [*Golledge et al*., 2012]. Additional details on the PISM model runs are available in *Fogwill et al*. [2014].

### 2.3. Internal Layer Continuity Index Plots

An Internal Layering Continuity Index (ILCI), derived from airborne radio echo sounding (RES) of the upper Institute Ice Stream catchment [*Winter et al*., 2015], was employed to characterize the internal stratigraphy of ice within Horseshoe Valley (using 100 trace moving windows), at predefined depth intervals of 0–20% (uppermost ice column), 40–60%, and 80–100% ice thickness. Developed by *Karlsson et al*. [2012] and recently applied to the Institute Ice Stream catchment by *Bingham et al*. [2015] and *Winter et al*. [2015], the ILCI uses relative changes in reflected radar power to assess the continuity of internal layers within the ice; this can provide insight into ice-flow history [*Bingham et al*., 2015]. Areas of high-reflected radar power, bounded by values of lower reflected relative power are recorded in A-scope plots of each RES trace (where each trace represents a stack of 10 consecutive raw traces to reduce noise) [*Karlsson et al*., 2012]. This allows areas of continuous internal layering to return a high ILCI (0.06–0.10), while absent and disrupted layers return a low ILCI ($>$0.06). These low to intermediate ILCI values have been interpreted to represent areas that have previously encountered or are currently experiencing enhanced flow (defined in this region as $>30\,\mathrm{m\,a^{-1}}$ [*Winter et al*., 2015]). Following *Winter et al*. [2015], we specify the term "enhanced flow" as distinct from the term "fast flow," as the latter term is often equated with more extreme ice speeds in ice streams.

## 3. Results

### 3.1. Ground-Penetrating Radar

GPR identified the following features in Patriot Hills BIA: blue ice with conformable steeply dipping internal stratigraphy; two pronounced divergent isochrones, associated with truncated layers; and blue ice that lacks strong internal stratigraphy at the start of transect A and profiles Y1–Y8 (Figures 2 and 3). The radar grid also shows a variety of features in the firn zone including truncated firn layers, prograding bedding sequences, surface-conformable stratigraphy, unconformities, firn that exhibits convergence, and surface snow drifts (Figure 3).

GPR Transect A (Figure 2), surveyed in step-and-collect mode, shows continuous, conformable, steeply dipping (inclined by 24°–45° toward Patriot Hills) isochrones from 0 m to 246 m, 249 m to 359 m, and 362 m to 800 m, where the internal reflectors strike from the lower ice column up toward the BIA surface. At 247 m and 360 m there are discontinuities in the isochrone layers (labeled D1 and D2, Figure 2b), where divergent isochrones represent significant changes in isochrone dip angle (Figure 2c). These discontinuities, associated with the truncation of isochrones, correlate to rapid changes in the trend of the deuterium isotopic record ($\delta$D) at approximately 18 cal ka and 12 cal ka [*Turney et al*., 2013]. B1 marks the transition from a low average $\delta$D rate to a rising trend in $\delta$D concentrations, where $\delta$D increases from $-380$ to $-254$‰. B2 marks a very rapid rise in $\delta$D concentrations from $-300$ to $-254$‰, after which a higher average ratio continues for the remainder of the profile. It has been suggested by *Turney et al*. [2013] that these changes, highlighted by shaded bands B1 and B2 in Figure 2d, could reflect significant changes in temperature and/or precipitation during both the late Pleistocene and Holocene [*Turney et al*., 2013]. There is, however, no evidence of divergent or truncated isochrones at any other location along the profile, even at B3 (~8 cal ka), where a depletion in deuterium isotope content is recorded.

Examples from the snowmobile-towed GPR grid, collected for wider analysis of the BIA and firn, are displayed in Figure 3 (inline Transects Y5 and Y7). Unlike GPR in step-and collect mode we detect limited internal features within the BIA using this method. However, numerous internal horizons are identified at the BIA/firn margin where a net upward ice flow component dominates the radargrams, with compressed isochrones inclined to a maximum dip angle of 5°. Each inline profile displays sequences of convergent and prograding isochrones within the firn zone which can be matched laterally between transects. An erosional unconformity is revealed in profile Y7 (Figure 3) where gently sloping (2° apparent dip toward Patriot Hills) internal horizons are overlain by younger, near horizontal firn layers between 2690 m and 3149 m along the transect, which more than double in thickness with increasing distance from Patriot Hills. A shallow snow drift is also visible in profile Y5 (Figure 3), near the BIA/firn margin where the 9 m thick drift extends 440 m along the former, near horizontal firn surface.

### 3.2. Ice Sheet Model Simulations

Simulated regional ice flux models show the initial response of the LGM ice sheet to ocean and atmospheric forcing where high discharge rates are simulated through all the major troughs, although no major ice flux or flow direction change is modeled in Horseshoe Valley (Figure 4a). With a rapid increase in ice flux in response to ocean

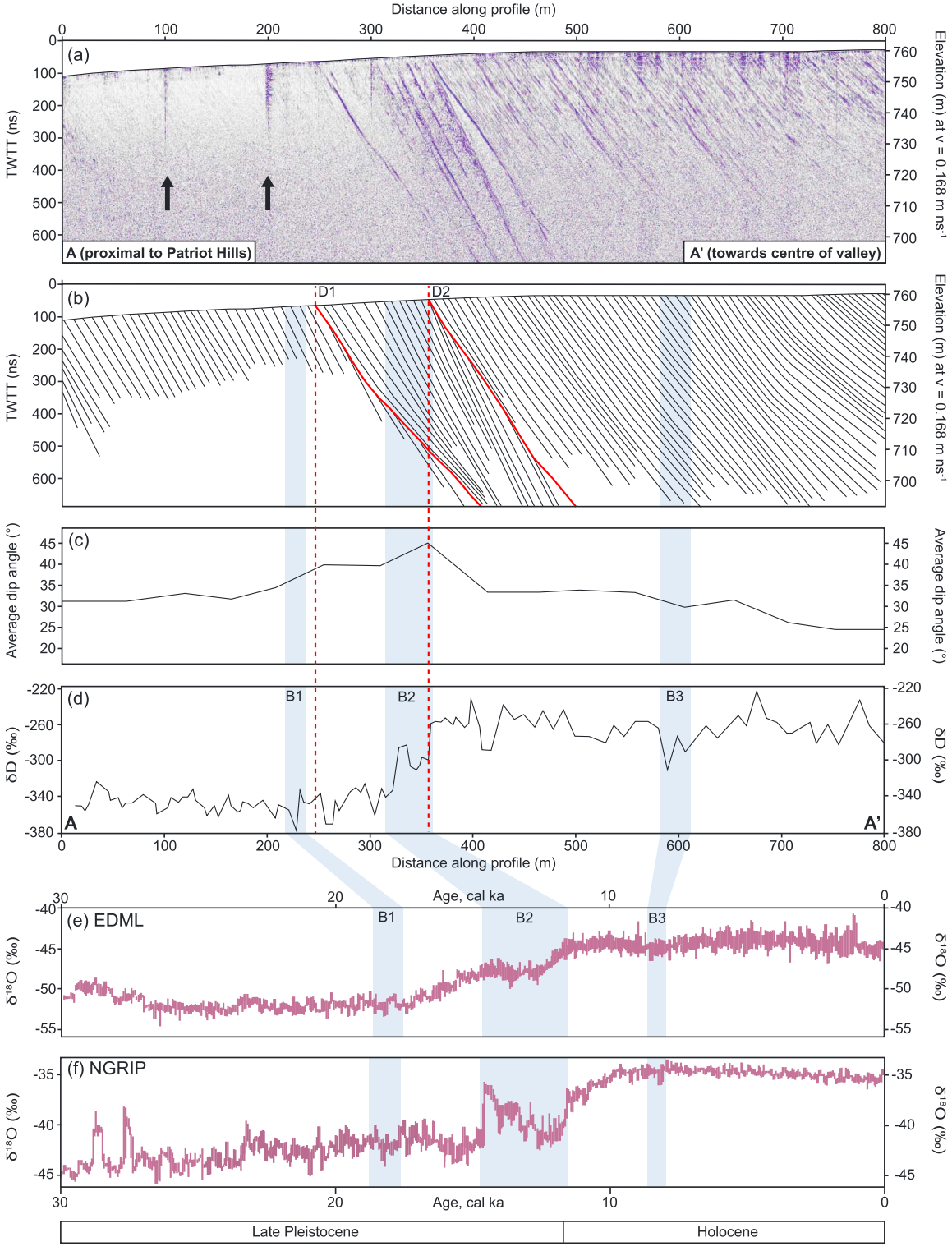


**Figure 2.** Ground-penetrating radar Transect A collected along the Blue Ice Area in front of Patriot Hills. (a) Elevation-corrected 200 MHz GPR profile recording the subsurface internal layer structure along a central transect extending from Patriot Hills (arrows indicate vertical noise from boreholes). (b) Picked, prominent internal GPR reflectors showing two locations where the internal reflectors are disturbed, i.e., showing changes in dip and discontinuity. D1 is at 247 m and D2 at 360 m along the transect. (c) Spatial variability of internal reflector dip angles in the along-line direction (averaged over 20 m intervals), and (d) Patriot Hills deuterium isotope record ($\delta$D) collected by *Turney et al.* [2013] in 2012. Shaded bands B1, B2, and B3 are inferred points of correlation with (e) the EPICA EDML $\delta^{18}$O record [*EPICA Community Members et al.*, 2006] (on the Greenland Ice Core Chronology 2005 time scale) and (f) the North Greenland ice core $\delta^{18}$O [*Rasmussen et al.*, 2006] as shown in Figure 4 of *Turney et al.* [2013].

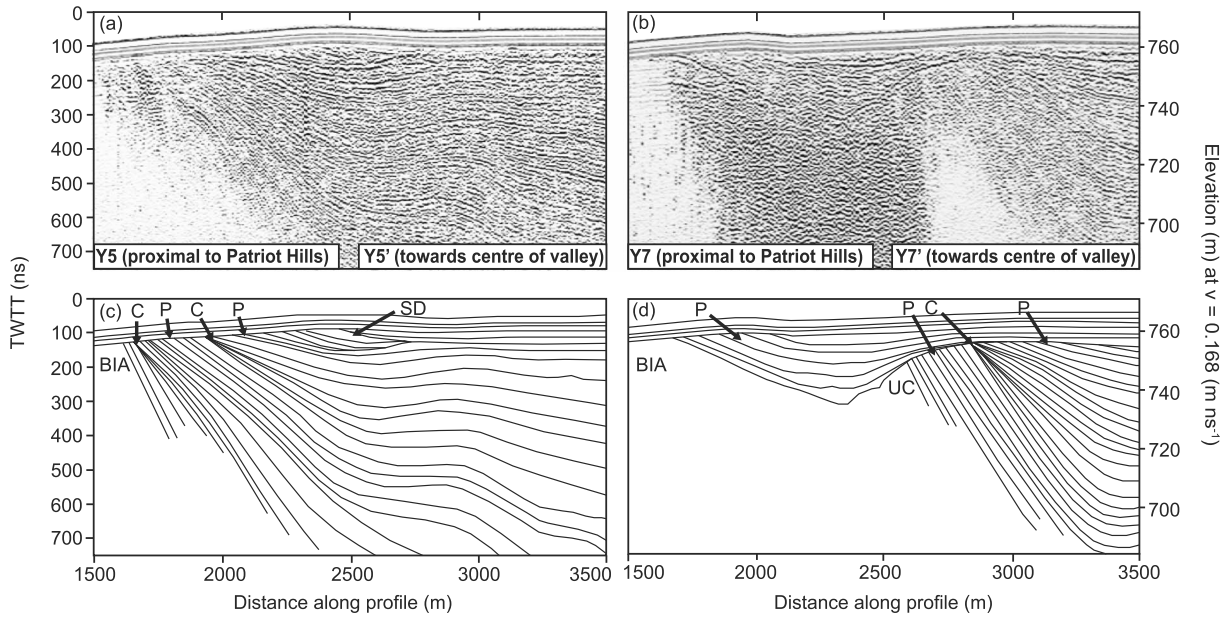


**Figure 3.** Snowmobile-towed 200 MHz ground-penetrating radar cross lines. (a) Elevation-corrected profile Y5. (b) Elevation-corrected profile Y7. (c) Picked, prominent internal GPR reflectors along Y5 show prograding (P) and convergent (C) isochrone sequences on approach to Patriot Hills Blue Ice Area (BIA), as well as a snow drift (SD). (d) Picked, prominent internal GPR reflectors along Y7 show prograding (P) and convergent (C) isochrone sequences as well as a stratigraphic unconformity (UC), where shallow dipping (2° apparent dip toward Patriot Hills) internal reflectors are overlain by younger near-horizontal firn layers.

forcing, modeled ice flowing into Institute Ice Stream continues to discharge through Rutford Trough (Figure 4b), even when flow accelerates at the ice margins. Continued oceanic forcing and grounding line retreat have no direct impact on the flow of ice around Patriot Hills, even when ice discharging into Institute Ice Stream is diverted in a more east-south-easterly direction toward the Thiel Trough (Figure 4c, bottom panel).

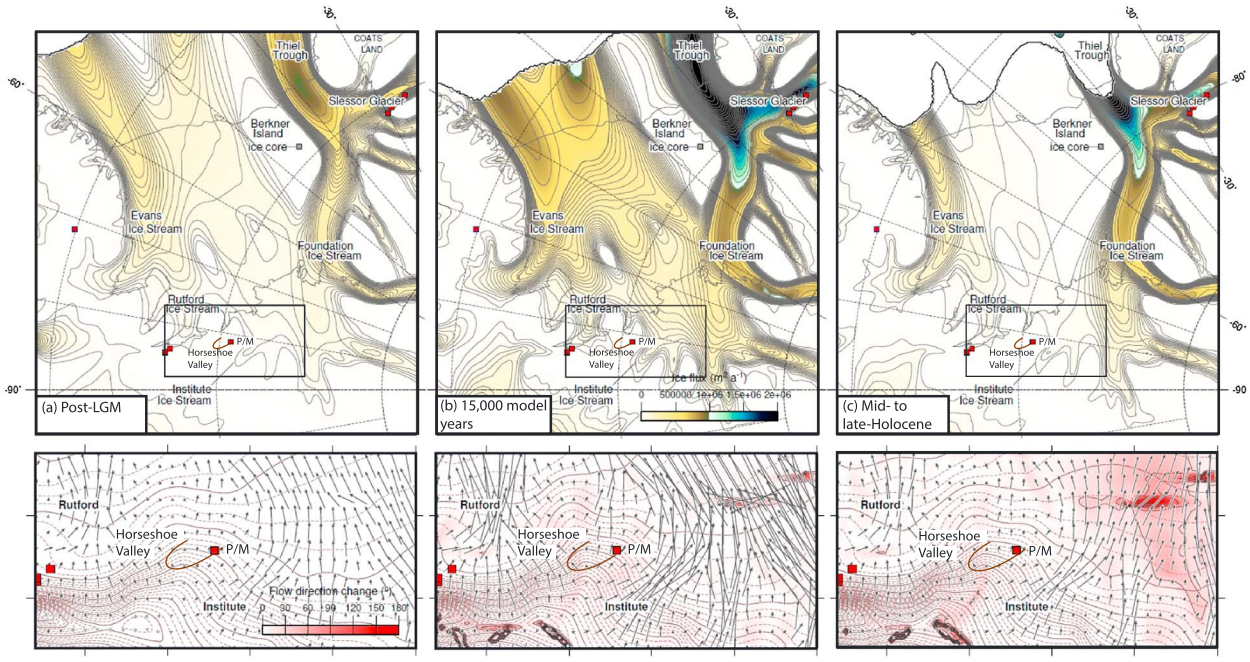


**Figure 4.** Simulated regional ice flux, generated from Parallel Ice Sheet Model simulations, capturing configurations representative of (a) post-LGM, (b) 15,000 model years, and (c) the Middle- to Late-Holocene response of the ice sheet to ocean and atmospheric forcing. Model results show that continued forcings do not impact the flow direction of ice around Patriot and Marble Hills, even when ice discharging into Institute Ice Stream is diverted in a more east-south-easterly direction toward Thiel Trough during the Middle to Late-Holocene (bottom panel of Figure 4c).

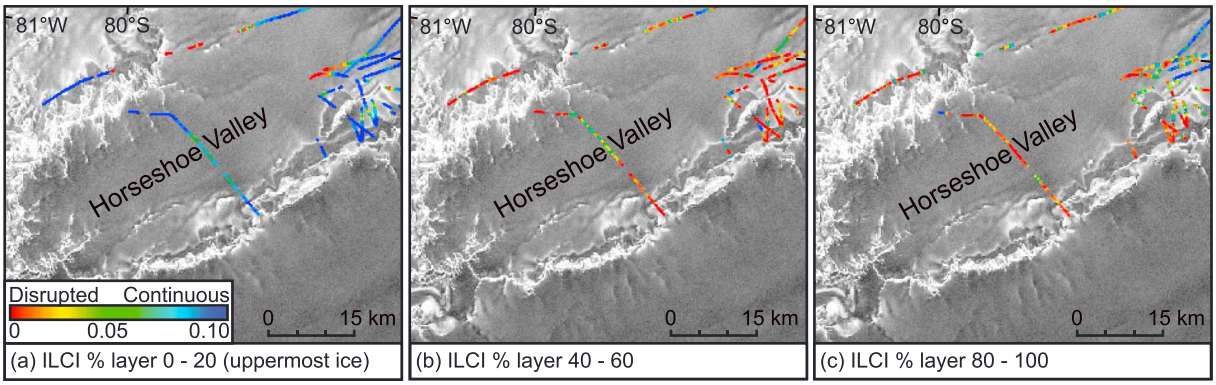


**Figure 5.** ILCI results from airborne RES flight lines across Horseshoe Valley (using 100 trace moving windows) at various depth intervals (a) % layer 0–20 reveals high ILCI values indicative of continuous layering in the uppermost ice column, (b) % layer 40–60 in the central ice column shows both continuous and disrupted internal layering, while (c) % layer 80–100 shows the most disrupted and discontinuous layering at depth. These plots, superimposed onto RADARSAT mosaic [*Haran et al.*, 2006], reveal that ice flow in Horseshoe Valley has been stable and slow flowing in recent years.

### 3.3. Internal Layer Continuity Index Plots

ILCI plots demonstrate that the uppermost ice in Horseshoe Valley (0–20% of the ice column) is dominated by continuous internal layering, indicative of slow flow, while older ice at 40–60% ice thickness and then 80–100% of the ice column return progressively higher ILCI values. Following *Winter et al.* [2015], these high ILCI values provide evidence for previously enhanced ice flow in Horseshoe Valley.

## 4. Discussion

Our GPR transects, ice sheet model simulations, and ILCI analyses each contribute to our understanding of ice sheet flow history in Horseshoe Valley and help to constrain the evolution of Patriot Hills BIA. Analysis of high-resolution GPR-detected internal stratigraphy reveals largely conformable isochrones which are inclined toward Patriot Hills BIA surface. Minor changes in the dip angle of the predominantly parallel internal horizons within the BIA do occur and are expected as a result of differential snow deposition, burial, and subsequent ice flow over time, but the pronounced changes in dip angles at D1 and D2 (Figure 2) represent larger scale change. These discontinuities correspond to abrupt shifts in the local climate record between ~18 cal ka (B1) and ~12 cal ka (B2) (Figure 2) and therefore represent breaks in an otherwise largely unbroken 30,000 year climate record. These breaks, given new context by the unconformities in GPR Transect A could have formed by one of two mechanisms: (1) changes in ice flowline trajectory or (2) local interaction of topography, snow accumulation, and wind.

Ice sheet model simulations and ILCI analysis suggest that ice in Horseshoe Valley has not experienced directional change (Figure 4) and has remained slow flowing (Figure 5) since the mid-Holocene. These findings eliminate the possibility that discontinuities D1 and D2 were formed by changes in ice flow-line trajectory but do not rule out significant periods of erosion. Periods of erosion could have resulted from the interaction of topography, snow accumulation, and wind as the ice flowed from the head of Horseshoe Valley toward Patriot Hills (Figure 6). We therefore expect that discontinuities D1 and D2, corresponding to changes in deuterium isotope concentrations at B1 and B2, were created by localized katabatic wind scour of the former snow and ice surface, as ice flowed through BIAs in front of Liberty and Marble Hills (Figure 6). Consequently, it seems probable that B1 and B2 do not directly represent abrupt climatic changes. As no other erosional events are found in the GPR record, it is assumed that other inferred depletions in the deuterium isotopes, such as that at B3, could reflect direct climatic changes during the early Holocene and indeed may correlate with changes in other ice cores [*Turney et al.*, 2013].

Our findings from the extended radar grid are in close agreement with the high-resolution BIA transect. Here the inline profiles show more recent periods of BIA stability and instability, reflected by convergent and prograding isochrones in the firn zone. Prograding isochrones in the GPR record (Figure 3) can be attributed to increased katabatic wind scour, and subsequent BIA expansion since the LGM. This is likely the result of surface lowering in Horseshoe Valley of up to ~480 m since the LGM [*Bentley et al.*, 2010], which would have revealed more of

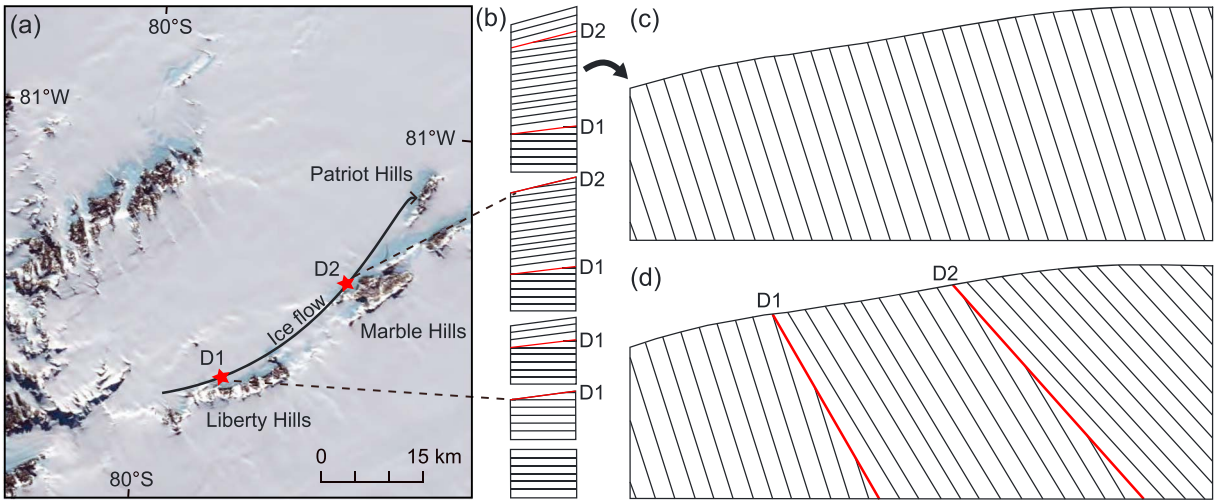


**Figure 6.** (a) Inferred ice flow path from the head of Horseshoe Valley to Patriot Hills (MODIS background image) [*Haran et al.*, 2006], where discontinuities D1 and D2 formed as a result of Blue Ice Area wind scour in front of Liberty and Marble Hills, (b) schematic stratigraphic succession, indicating ice accumulation punctuated by two periods of erosion (red lines), (c) lowermost Figure 6b rotated 90° to show an inferred cross section of unbroken snow/firn stratigraphy and, (d) uppermost panel of Figure 6b rotated to show the observed GPR stratigraphic sequence at Patriot Hills BIA, where red lines indicate erosional events D1 and D2.

the nunataks in the Southern Heritage Range, capable of promoting stronger katabatic wind scour. In contrast, younger convergent isochrones in the GPR record (Figure 3) represent more stable meteorological conditions, where katabatic winds of consistent velocity and direction have produced a transition zone between all annual snowfalls to no snowfall scoured. If these transition zones are in the same location annually, convergent layering will result. This also requires slow and stable ice sheet flow. These sequences of BIA growth and stabilization combine to identify an evolving BIA over the past ~1000 years, which is consistent with the previously analyzed 30,000 year ice flow records. The unconformable surface firn in profile Y7 and the snow drift in profile Y5 (Figure 3) have anthropogenic origins which are attributed to the recent movement of snow to create Patriot Hills Antarctic Logistics and Expeditions Base Camp (seasonally occupied between 1987 and 2010).

## 5. Conclusions

Radar-detected stratigraphic relationships analyzed in conjunction with deuterium isotope records, ice sheet model simulations, and internal layer continuity analysis at the Patriot Hills Blue Ice Area (BIA), West Antarctica, indicate the following: (1) stable periods of snow accumulation and ice flow have been interrupted by episodes of significant erosion, which have resulted in unconformities within the otherwise conformable stratigraphic record and (2) the current trajectory of ice flowing toward Patriot Hills BIA is, in essence, unchanged over the historical record. We conclude that deuterium isotope records from Patriot Hills BIA reflect conditions in Horseshoe Valley (and the West Antarctic Ice Sheet) over at least the last 30,000 years, though due consideration must be taken around the two periods of differential wind scour.

Importantly, this study also demonstrates the considerable value of using GPR in step-and-collect-mode to interpret ice sheet history from BIAs, as conventional snowmobile towed GPR cannot resolve the detailed internal structure of these ice features. This finding is particularly relevant to the climate community, as low-cost and portable GPR surveys in step-and-collect mode can greatly improve the reliability of relatively easily accessible horizontal climate records.

**Acknowledgments**
Project work was funded by NERC-standard grants NE/I027576/1, NE/I025840/1, NE/I024194/1, and NE/I025263/1 and Australian Research Council grants FL100100195, FT120100004, and LP120300724. Airborne radar data used for the ILCI analysis were acquired by NERC Antarctic Funding Initiative grant NE/G013071/1. We thank the British Antarctic Survey and Antarctic Logistics and Expeditions (ALE) for field and logistics support. The useful comments and advice of the referees and Editor are also gratefully acknowledged. Data used in this article will be made available on the NERC Geophysics Data Portal (geoportal.nerc-bas.ac.uk/GDP) and Northumbria University's institutional repository (nrl.northumbria.ac.uk) upon publication.

## References

Bentley, M. J., C. J. Fogwill, A. M. Le Brocq, A. L. Hubbard, D. E. Sugden, T. J. Dunai, and S. P. H. T. Freeman (2010), Deglacial history of the West Antarctic Ice Sheet in the Weddell Sea embayment: Constraints on past ice volume change, *Geology*, *38*, 411–414, doi:10.1130/G30754.1.

Bingham, R. G., D. M. Rippin, N. B. Karlsson, H. F. J. Corr, F. Ferraccioli, T. A. Jordan, A. M. Le Brocq, K. C. Rose, N. Ross, and M. J. Siegert (2015), Ice-flow structure and ice-dynamic changes in the Weddell Sea sector of West Antarctica from radar images internal layering, *J. Geophys. Res. Earth Surf.*, *120*, 655–670, doi:10.1002/204JF003291.

Bintanja, R. (1999), On the glaciological, meteorological, and climatological significance of Antarctic Blue Ice Areas, *Rev. Geophys.*, *37*(3), 337–359, doi:10.1029/1999RG900007.

Campbell, S., G. Balco, C. Todd, H. Conway, K. Huybers, C. Simmons, and M. Vermeulen (2013), Radar detected englacial stratigraphy in the Pensacola Mountains, Antarctica: Implications for recent changes in ice flow and accumulation, *Ann. Glaciol.*, *54*(63), 91–100, doi:10.3189/2013AoG63A371.

Clark, P. U., A. S. Dyke, J. D. Shakun, A. E. Carlson, J. Clark, B. Wohlfarth, J. X. Mitrovica, S. W. Hostetler, and A. M. McCabe (2009), The Last Glacial Maximum, *Science*, *325*, 710–714, doi:10.1126/science.1172973.

Daniels, D. J., D. J. Guton, and H. F. Scott (1988), Introduction to subsurface radar, *IEEE Proc.*, *135*(F4), 278–305.

Drews, R., C. Martín, D. Steinhage, and O. Eisen (2013), Characterizing the glaciological conditions at Halvfarryggen ice dome, Dronning Maud Land, Antarctica, *J. Glaciol.*, *59*(213), 9–20, doi:10.3189/2013JoG12J134.

EPICA Community Members, et al. (2006), One-to-one coupling of glacial climate variability in Greenland and Antarctica, *Nature*, *444*, 195–198, doi:10.1038/nature05301.

Fogwill, C. J., A. S. Hein, M. J. Bentley, and D. E. Sugden (2012), Do blue-ice moraines in the Heritage Range show the West Antarctic ice sheet survived the last interglacial? *Palaeogeogr. Palaeoclimatol. Palaeoecol.*, *335–336*, 61–70, doi:10.1016/j.palaeo.2011.01.027.

Fogwill, C. J., C. S. M. Turney, N. R. Golledge, D. H. Rood, K. Hippe, L. Wacker, R. Wieler, E. B. Rainsley, and R. S. Jones (2014), Drivers of abrupt Holocene shifts in West Antarctic ice stream direction determined from combined ice sheet modelling and geologic signatures, *Antarct. Sci.*, *26*(6), 674–686, doi:10.1017/S0954102014000613.

Fujita, S., H. Maeno, S. Uratsuka, T. Furukawa, S. Mae, Y. Fujii, and O. Watanabe (1999), Nature of radio echo layering in the Antarctic Ice Sheet detected by a two-frequency experiment, *J. Geophys. Res.*, *104*(B6), 13,013–13,024, doi:10.1029/1999JB900034.

Golledge, N. R., C. J. Fogwill, A. N. Mackintosh, and K. M. Buckley (2012), Dynamics of the Last Glacial Maximum Antarctic ice-sheet and its response to ocean forcing, *Proc. Natl. Acad. Sci. U.S.A.*, *109*(40), 16,052–16,056, doi:10.1073/pnas.1205385109.

Haran, T., J. Bohlander, T. Scambos, T. Painter, and M. Fahnestock (2006), *MODIS Mosaic Image of Antarctica*, National Snow and Ice Data Center, Boulder, Colo., Digital media.

Imbrie, J. D., and A. Mcintyre (2006), SPECMAP time scale developed by Imbrie et al. 1984 based on normalized planktonic records (normalized O-18 vs time, specmap.017), *Earth Syst. Sci. Data*, doi:10.1594/PANGAEA.441706.

Karlsson, N. B., D. M. Rippin, R. G. Bingham, and D. G. Vaughan (2012), A "continuity index" for assessing ice-sheet dynamics from radar-sounded internal layers, *Earth Planet. Sci. Lett.*, *335–336*, 88–94, doi:10.1016/j.epsl.2012.04.034.

King, E. C. (2011), Ice stream or not? Radio-echo sounding of Carlson Inlet, West Antarctica, *Cryosphere*, *5*(4), 907–916, doi:10.5194/tc-5-907-2011.

Korotkikh, E. V., P. A. Mayewski, M. J. Handley, S. B. Sneed, D. S. Introne, A. V. Kurbatov, N. W. Dunbar, and W. C. McIntosh (2011), The last interglacial as represented in the glaciochemical record from Mount Moulton Blue Ice Area, West Antarctica, *Quat. Sci. Rev.*, *30*, 1940–1947, doi:10.1016/j.quascirev.2011.04.020.

Le Brocq, A. M., A. J. Payne, and A. Vieli (2010), An improved Antarctic dataset for high resolution numerical ice sheet models (ALBMAP v1), *Earth Syst. Sci. Data*, *2*, 247–260, doi:10.5194/essd-2-247-2010.

Lisiecki, L. E., and M. E. Raymo (2005), A Pliocene-Pleistocene stack of 57 globally distributed benthic 18O records, *Paleoceanography*, *20*, PA1003, doi:10.1029/2004PA001071.

Paren, J. G., and G. de Q. Robin (1975), Internal reflections in polar ice sheets, *J. Glaciol.*, *14*(71), 251–259.

Petit, J. R., et al. (1999), Climate and atmospheric history of the past 420,000 years from the Vostok ice core, Antarctica, *Nature*, *399*, 429–436, doi:10.1038/20859.

Rasmussen, S. O., et al. (2006), A new Greenland ice core chronology for the last glacial termination, *J. Geophys. Res.*, *111*, D06102, doi:10.1029/2005JD006079.

Rippin, D. M., M. J. Siegert, and J. L. Bamber (2003), The englacial stratigraphy of Wilkes Land, East Antarctica, as revealed by internal radio-echo sounding layering and its relationship with balance velocities, *Ann. Glaciol.*, *36*, 189–196, doi:10.3189/172756403781816356.

Rippin, D. M., M. J. Siegert, J. L. Bamber, D. G. Vaughan, and H. F. J. Corr (2006), Switch off of a major enhanced ice flow unit in East Antarctica, *Geophys. Res. Lett.*, *33*, L15501, doi:10.1029/2006GL026648.

Sandmeier Scientific Software (2012), ReflexW, version 6.1.1. [Available at http://www.sandmeier-geo.de/download.html.]

Shapiro, N. M., and M. H. Ritzwoller (2004), Inferring surface heat flux distributions guided by a global seismic model: Particular application to Antarctica, *Earth Planet. Sci. Lett.*, *223*, 213–224, doi:10.1016/j.epsl.2004.04.011.

Sime, L. C., R. C. Hindmarsh, and H. F. J. Corr (2011), Instruments and Methods: Automated processing to derive dip angles of englacial radar reflectors in ice sheets, *J. Glaciol.*, *57*, 260–266, doi:10.3189/002214311796405870.

Sinisalo, A., and J. C. Moore (2010), Antarctic Blue Ice Areas—Towards extracting paleoclimate information, *Antarct. Sci.*, *22*(02), 99–115, doi:10.1017/S0954102009990691.

Spaulding, N. E., V. B. Spikes, G. S. Hamilton, P. A. Mayewski, W. Nelia, R. P. Harvey, J. Schutt, and A. V. Kurbatov (2012), Ice motion and mass balance at the Allan Hills blue ice area, Antarctica, with implications for paleoclimate reconstructions, *J. Glaciol.*, *58*, 399–406, doi:10.3189/2012JoG11J176.

Spaulding, N. E., J. A. Higgins, A. V. Kurbatov, M. L. Bender, S. A. Arcone, S. Campbell, N. W. Dunbar, L. M. Chimiak, D. S. Introne, and P. A. Mayewski (2013), Climate archives from 90 to 250 ka in horizontal and vertical ice cores from the Allan Hills Blue Ice Area, Antarctica, *Quat. Res.*, *80*, 562–574, doi:10.1016/j.yqres.2013.07.004.

Turney, C., C. Fogwill, T. D. Van Ommen, A. D. Moy, D. Etheridge, M. Rubino, and A. Rivera (2013), Late Pleistocene and early Holocene change in the Weddell Sea: A new climate record from the Patriot Hills, Ellsworth Mountains, West Antarctica, *J. Quat. Sci.*, *28*(7), 697–704, doi:10.1002/jqs.2668.

Welch, B. C., and R. W. Jacobel (2005), Bedrock topography and wind erosion sites in East Antarctica: Observations from the 2002 US-ITASE traverse, *Ann. Glaciol.*, *41*, 92–96, doi:10.3189/172756405781813258.

Whillans, I. M., and W. A. Cassidy (1983), Catch a falling star: Meteorites and old ice, *Science*, *222*, 55–57.

Winter, K., J. Woodward, N. Ross, S. A. Dunning, R. G. Bingham, H. F. J. Corr, and M. J. Siegert (2015), Airborne radar evidence for tributary flow switching in Institute Ice Stream, West Antarctica: Implications for ice sheet configuration and dynamics, *J. Geophys. Res. Earth Surf.*, *120*, 1611–1625, doi:10.1002/2015JF003518.

Winther, J.-G., M. Jespersen, and G. Liston (2001), Blue-ice areas in Antarctica derived from NOAA AVHRR satellite data, *J. Glaciol.*, *47*(157), 325–334, doi:10.3189/172756501781832386.

Woodward, J., and E. C. King (2009), Radar surveys of the Rutford Ice Stream onset zone, West Antarctica: Indications of flow (in)stability? *Ann. Glaciol.*, *50*(51), 57–62, doi:10.3189/172756409789097469.

Woodward, J., P. J. Ashworth, J. L. Best, G. H. Sambrook Smith, and C. J. Simpson (2001), The use and application of GPR in sandy fluvial environments: Methodological considerations, in *Ground Penetrating Radar in Sediments*, vol. 211, edited by C. S. Bristow and H. M. Jol, 211, pp. 127–142, *Geol. Soc. Spec. Publ.*, doi:10.1144/GSL.SP.2001.211.01.11.